Clim Dyn (2013) 41:551–571
DOI 10.1007/s00382-013-1823-8

Winter weather regimes over the Mediterranean region: their role for the regional climate and projected changes in the twenty-first century

M. Rojas · L. Z. Li · M. Kanakidou · N. Hatzianastassiou · G. Seze · H. Le Treut

Received: 23 November 2011 / Accepted: 28 May 2013 / Published online: 30 June 2013

Abstract The winter time weather variability over the Mediterranean is studied in relation to the prevailing weather regimes (WRs) over the region. Using daily geopotential heights at 700 hPa from the ECMWF ERA40 Reanalysis Project and Cluster Analysis, four WRs are identified, in increasing order of frequency of occurrence, as cyclonic (22.0 %), zonal (24.8 %), meridional (25.2 %) and anticyclonic (28.0 %). The surface climate, cloud distribution and radiation patterns associated with these winter WRs are deduced from satellite (ISCCP) and other observational (E-OBS, ERA40) datasets. The LMDz atmosphere–ocean regional climate model is able to simulate successfully the same four Mediterranean weather regimes and reproduce the associated surface and atmospheric conditions for the present climate (1961–1990). Both observational- and LMDz-based computations show that the four Mediterranean weather regimes control the region's weather and climate conditions during winter, exhibiting significant differences between them as for temperature, precipitation, cloudiness and radiation distributions within the region. Projections (2021–2050) of the winter Mediterranean weather and climate are obtained using the LMDz model and analysed in relation to the simulated changes in the four WRs. According to the SRES A1B emission scenario, a significant warming (between 2 and 4 °C) is projected to occur in the region, along with a precipitation decrease by 10–20 % in southern Europe, Mediterranean Sea and North Africa, against a 10 % precipitation increase in northern European areas. The projected changes in temperature and precipitation in the Mediterranean are explained by the model-predicted changes in the frequency of occurrence as well as in the intra-seasonal variability of the regional weather regimes. The anticyclonic configuration is projected to become more recurrent, contributing to the decreased precipitation over most of the basin, while the cyclonic and zonal ones become more sporadic, resulting in more days with below normal precipitation over most of the basin, and on the eastern part of the region, respectively. The changes in frequency and intra-seasonal variability highlights the usefulness of dynamics versus statistical downscaling techniques for climate change studies.

Keywords Mediterranean · Winter weather regimes · Climate change · Coupled regional atmosphere–ocean simulation

Electronic supplementary material The online version of this article (doi:10.1007/s00382-013-1823-8) contains supplementary material, which is available to authorized users.

M. Rojas (✉)
Department of Geophysics, University of Chile, Santiago, Chile
e-mail: maisa@dgf.uchile.cl

M. Rojas · L. Z. Li · G. Seze · H. Le Treut
LMD/IPSL/CNRS, Université Paris 6, 4 place Jussieu, 75252 Paris Cedex 05, France

M. Kanakidou
Environmental Chemical Processes Laboratory, Chemistry Department, University of Crete, 71003 Heraklion, Greece

N. Hatzianastassiou
Laboratory of Meteorology, Physics Department, University of Ioannina, 45110 Ioannina, Greece

1 Introduction

The Mediterranean region consists of a landmass surrounding a body of saline water (Mediterranean Sea) that is

a semi-enclosed marginal sea with a narrow strait at Gibraltar in communication with the rest of the oceans. The typical Mediterranean climate, which lies between the semi-arid climate of North Africa and the temperate and rainy climate of central Europe, is characterized by hot, dry summers and mild, rainy winters. Evaporation exceeds largely precipitation and river runoff in this region (Mariotti et al. 2008), which makes the Mediterranean Sea a concentration basin. The winter Mediterranean climate, especially in terms of precipitation, is significantly influenced by the westerlies and the associated cyclonic activity, and by the North Atlantic Oscillation (NAO) that affect more the western (e.g. Hurrell 1996) than the eastern parts (Alpert et al. 2006; Hatzianastassiou et al. 2009). The East Atlantic (EA) oscillation also impacts the northern and eastern areas of the Mediterranean (Trigo et al. 2006). In addition to Atlantic storms, Mediterranean storms can be generated within the region through cyclogenesis in areas such as the lee of the Alps, the Gulf of Lyon and the Gulf of Genoa (Lionello et al. 2006a).

As a consequence of its location in a transition zone between humid mid-latitude and semiarid subtropics, the Mediterranean is a climatically sensitive region. It is often exposed to multiple stresses, such as a simultaneous water shortage and air pollution exposure (IPCC 2007) that affect the population of the countries surrounding the Mediterranean Sea. The Mediterranean climate is vulnerable to changes caused either by anthropogenic forcings, like increases in concentrations of greenhouse gases (e.g. Lionello et al. 2006b; Ulbrich et al. 2006) or changes in atmospheric aerosols (Alpert et al. 2006), as well as by natural forcings, like variability of the position and strength of the mid-latitude storm tracks or sub-tropical cells (Giorgi and Lionello 2008). The large sensitivity of Mediterranean climate has been seen by significant climatic shifts that took place in the past (Luterbacher et al. 2006) and are expected to occur in the future since the region has been identified as one of the "hot spots" of future climate change (Giorgi 2006). The strong atmospheric variability over Europe and the Mediterranean region is even higher in winter (e.g. Xoplaki et al. 2004; Jones and Lister 2009) and impacts on life and economic development.

Investigation of persistent and recurrent large-scale flow patterns that appear repeatedly at fixed geographical locations, known as weather regimes (WRs), can contribute to illuminate the climate variability of the Mediterranean region. WRs organize the behaviour of synoptic systems that affect local-scale weather during several days or even consecutive weeks (Ullmann and Moron 2008). Therefore, WRs can explain many aspects of local weather and climate over different regions, not only in terms of mean but also in terms of variability and extremes (Yiou et al. 2006). Weather regimes have been largely used to characterize the atmospheric dynamic circulation patterns (Michelangeli et al. 1995) relevant to weather conditions for most of mid-latitude regions, Northern Hemisphere (Corti et al. 1999; Straus and Molteni 2004); Southern Hemisphere (Solman and Menendez 2003) and Europe (Vautard 1990; Moron and Plaut 2003). For example, Ullmann and Moron (2008) analyzed observed sea surge variations over the French Mediterranean coast, and found five WRs over the northeast Atlantic and Europe during wintertime periods of the twentieth century (1905–2002). They found that more than 75 % of sea surges $\geq$ 40 cm occurred during WRs associated with a negative NAO phase. Santos et al. (2005) performed a similar study over Portugal in order to isolate the WRs responsible for the interannual variability of the winter precipitation and found this was strongly coupled with the large-scale atmospheric flow in the Euro-Atlantic sector. Fontaine et al. (2011) examined the relationship between WRs over the Euro-Mediterranean region and West Africa rainfall, and found that changes in WR frequencies account for a part of the West Africa's inter-annual rainfall variability. Vrac and Yiou (2010) provide a comprehensive review of clustering algorithms for local precipitation modelling over the Mediterranean basin, discussing the pros and cons of several methods, with an emphasis on extreme precipitation events. In a recent study, Beaulant et al. (2011) apply the k-means cluster method to identify large-scale circulation patterns associated to extreme precipitation events in Southern France in the present and future, and find an increase in heavy precipitation events under SRES A2 scenario by the end of the century in this region.

The scope of the present work is to study the spatio-temporal variability of cloud cover and surface climate parameters over the Mediterranean region during winter in relation with the main synoptic configuration affecting the region that define distinct WRs, to evaluate the ability of an atmosphere–ocean coupled regional climate model (LMDz) to simulate this variability and to analyze future wintertime climate projections for the Mediterranean. Particular emphasis is placed on investigating how cloud properties vary as function of dynamical atmospheric circulation regimes over the Mediterranean. To achieve this, first, the main wintertime WRs of the region are determined based on 700 hPa geopotential height (Z700) data from the European reanalysis Project ERA40. Then, the variability of these regional WRs is investigated in relation to associated key meteorological variables, namely surface air-temperature, precipitation, total cloudiness and surface shortwave and longwave radiation fields. Data from ground based observations, ERA40 Reanalysis, and satellite ISCCP database, are used here. This study focuses on winter because during winter the Mediterranean climate variability maximizes and because winter contributes the largest part of annual mean regional cloudiness and precipitation.

To assess WRs in the Mediterranean region and their potential changes in a climate change scenario, we have used the atmospheric–ocean coupled regional climate model LMDz. The simulation is 100 years long (1951–2050) covering recent and future climate, following the SRES A1B emission scenario.

The remainder of the paper is organized as following. Section 2 gives a brief outline of the LMDz model and the datasets used for model evaluation and for weather regime analysis. The clustering method applied for the determination of the weather regimes is given in Sect. 3. Section 4 presents the climatological wintertime conditions in the Mediterranean (4.1) and then analyzes the results of the clustering applied to ERA40 and to LMDz (4.2). An analysis of clouds in LMDz is given in Sect. 4.3. In Sect. 4.4, the 2021–2050 projected changes in WRs are discussed. Finally Sect. 5 provides a summary and conclusions.

2 Models and datasets

2.1 LMDz/NEMO-MED8 model

The regional coupled model used in this study is composed of the LMDZ-regional atmospheric (Li 1999; Hourdin et al. 2006) and NEMO-MED8 oceanic models. LMDZ-regional is an atmospheric general circulation model, with a zoom over the Mediterranean region. The spatial resolution over the Mediterranean basin is about 30 km. LMDz is used here as a traditional regional climate model (RCM), since it is forced, outside the Mediterranean domain every 6-h, by outputs of the IPSL-CM4 global ocean–atmosphere coupled model (Marti et al. 2010). NEMO-MED8, described by Sevault et al. (2009), is an oceanic general circulation model operated for the Mediterranean Sea. Its horizontal resolution is 1/8 degree (that corresponds to about 10.6 km at 40°N and 11.4 km at 35°N) and with 43 layers in the vertical from the sea-surface to the bottom.

A small area of the North Atlantic near the Strait of Gibraltar is taken into account in the model as a buffer zone. In this zone, both temperature and salinity are relaxed to values calculated by the coarse resolution global oceanic model, and the net inflow from the Atlantic Ocean is about 0.06 Sv. The Black Sea is neglected and is only considered as a source of fresh water, with a climatological seasonal cycle. The LMDZ-regional and NEMO-MED8 models are interactively coupled through the coupler OASIS (Valcke, 2006) at a diurnal frequency. For each day, LMDZ-regional provides the surface radiative fluxes, turbulent heat fluxes and wind stress to NEMO-MED8 and receives in turn the sea-surface temperature (SST). Heat fluxes and SST are interpolated through a simple re-mapping scheme, which conserves the domain average. Wind stress is interpolated by a bilinear scheme that has a good behaviour in dealing the curl of winds.

The initial state of the Mediterranean Sea is set to the climatology of Medatlas (Mediterranean and Black Sea Database of temperature, salinity and bio-chemical parameters climatological atlas, MEDATLAS 1997) for January in terms of oceanic temperature and salinity, and there are no currents at the initialisation. The spin-up of the coupled model has a duration of 30 years. After the spin-up time, the regional coupled model is run with outputs of IPSL-CM4 under historical conditions (solar constant, greenhouse gases, sulphate aerosols and volcanism) from 1951 to 2000, and under the IPCC SRES-A1B scenario from 2001 to 2050.

2.2 ISCCP dataset

We use the "International Satellite Cloud Climatology Project" (ISCCP) D1 dataset to evaluate winter cloudiness over the Mediterranean region. The ISCCP D1 (Rossow and Schiffer 1999; http://isccp.giss.nas.gov) provides a global distribution of cloud amount and other properties (cloud-top altitude and optical thickness) at 280 × 280 km^2 scale and 3-h intervals from 1983 to present. The ISCCP data set is built from measurements of the visible and infrared multi-spectral radiometers on board five geostationary and two polar orbiting operational weather satellites. The cloud parameters (Rossow et al. 1996) are inferred from the analysis of the visible (daytime) and infrared (night time and daytime) full resolution data (ranging from 4 km to 7 km) and sampled to 30 km spacing. At low and mid-latitudes, to attain global uniformity in the multi-satellite data set, the number of channels used has been restrained to one visible channel and one IR window channel.

The cloud identification is performed with a threshold technique using IR (night-time and daytime) and VIS (daytime) clear-sky values; these values are established from statistical analysis of the spatial and temporal variability of the data (Rossow and Garder 1993). For daytime data, both IR and VIS/IR cloud fractions (number of full resolution pixel identified as cloud contaminated) are available; this allows insight into the bias of the night-time cloud fraction compared to the VIS/IR daytime cloud fraction. During daytime, the VIS data allow improved detection of low clouds.

The retrieved ISCCP daytime cloud cover is within the 68 % (±3 %) of other cloud cover climatologies, when the sub-visual clouds with optical thickness smaller than 0.1 (about 5 % of the CALIOP lidar observations) are not considered (Stubenrauch et al. 2012). Taking into account the sub-visual high-level clouds (OD < 0.1) detected only with the CALIOP lidar, increases the cloud cover amount by more than 10 % in the tropics (15°N–15°S), but by less than 5 % in

the northern hemisphere mid-latitudes. The latitudinal, regional and seasonal variations of the ISCCP cloud cover amount are in agreement with the other climatologies (Stubenrauch et al. 2012; Rossow and Golea 2013).

In the present study, the ISCCP D1 data for the period from March 1983 to February 2000 and the region 10°W–35°E and 25°N–50°N are used. This region is entirely within the field of view of the METEOSAT geostationary satellite, avoiding thus discontinuities that may arise from changes in instruments. For each day the cloud cover field at 12GMT has been retained since visible observations are available for the whole region at this time.

2.3 Era40

Various fields from the European Reanalysis project ERA40 (Uppala et al. 2005), produced by ECMWF are used in this study. ERA40 is a globally gridded dataset of horizontal (spectral) resolution T159 (about 125 km) and 60 vertical levels, and covers the period 1958–2001. To calculate the weather regimes we have used the daily geopotential height at 700 hPa (Z700). Upward and downward shortwave and longwave radiation fields at the surface have also been analysed to characterise the 4 identified regimes, and to evaluate radiation fields from the LMDz model.

For Sea surface temperature comparison we have used the monthly version of HadISST 1.1 Sea Surface Temperature dataset (Rayner et al. 2002).

2.4 E-OBS dataset

The E-OBS (Haylock et al. 2008), part of the European Climate Assessment and Dataset (ECA&D), is a European land-only high-resolution gridded data set for daily precipitation and surface minimum, maximum, and mean daily temperature for the period 1950–2006. The data set was developed as part of the European Union Framework 6 ENSEMBLES project for validation of Regional Climate Models and for climate change studies. This gridded data set has been produced by interpolating more than 2300 station data over the region, using a three steps "kriging" procedure. The dataset includes daily estimates of the interpolation uncertainty, provided as standard error, which, although not the only one, constitutes the largest source of uncertainty in the dataset. In the present study we use the 50 km gridded E-OBS product.

3 Methodology

In order to determine the characteristic weather regimes prevailing over the Mediterranean, we apply a clustering method to daily 700 hPa geopotential height (Z700) over the domain shown in Fig. 1. The level of 700 hPa was chosen as being representative of the lower layer of the atmosphere, where most weather phenomena take place. The clustering method is k-means (e.g. MacQueen 1967), one of the simplest unsupervised learning algorithms that solve the well-known clustering problem.

The procedure follows a simple and easy way to classify a given data set into a certain number of clusters (assume k clusters) that are fixed a priori. The main idea is to define k centroids, one for each cluster. The next step is to associate each point of a given data set to the nearest centroid. When no point is pending, the first step is completed and an early grouping is done. At this point k new centroids are re-calculated as barycenters of the clusters resulting from the previous step. After determining these k new centroids, a new binding has to be done between the same data set points and the nearest new centroid. In this way, a loop is being generated, and the k centroids may change their location step by step. When no more changes are done, i.e. centroids do not move any more, the procedure is completed and the final clustering is obtained. Although it can be proved that the procedure is always terminated, the k-means algorithm does not necessarily find the minimum of the function to be minimized, i.e. mean intra-cluster variance. The algorithm is also significantly sensitive to the initial randomly selected cluster centres.

In this work, we use the k-means function implemented in matlab, and the number of clusters is fixed at 4. The choice of 4 clusters is justified by three independent considerations.

We repeated the k-means clustering algorithm with $k = 2$–8, and, to ensure a stable solution of the clustering algorithms, we repeated the procedure 100 times. For $k = 4$, less than 1 % of the individual days fall into a different cluster when repeating the calculation, hence producing a very stable result. For 3–8 initially set clusters the stability falls to 10–30 %, to the point that for 8 clusters no convergence is found (not shown). A second approach to evaluate the robustness of the clustering results, in relation to other initial number of clusters, was to apply the Silhouette Validation Method (Rousseeuw 1987). This method represents each cluster by a so-called "silhouette" that compares the tightness and separation with respect to other choices of cluster number. Applying this validation procedure for 2–8 clusters, we found largest value of this index (i.e., goodness of cluster separation) is for 2 clusters, and second largest validity for 4 clusters.

Finally, previous work using similar clustering methods to study wintertime climate in Europe have diagnosed 4 clusters as the number to group weather regimes (Nuissier et al. 2011). Vrac and Yiou (2010) use 7 clusters, but four of those correspond closely to clusters found in this study (see their Fig. 10). Notice that Vrac and Yiou, like many

other WRs studies use 500 hPa geopotential height to calculate the regimes, unlike Plaut and Simmonnet (2001) for example or our study that use Z700.

In summary, in this work, we use the k-means function implemented in matlab, and the number of clusters is fixed at 4. The cluster calculation was performed over the winter period 1961–2002.

Both ERA40 and LMDz daily Z700 fields were first detrended. We assumed a linear trend that was subtracted from the field at each grid-point, and then the seasonal cycle was removed. Finally, to make the clustering calculation more efficient, we use also a principal component analysis and keep the first 10 components. The detrending procedure is especially important for the LMDz fields, since the clustering analysis is done for the complete length (100 years) of the simulation, and LMDz has a significant positive trend in the Z700 field throughout the complete simulation (due to global warming). The same procedure was applied to ERA40 for consistency.

The present work investigates the winter time WR (DJF). The k-means clustering method is applied to the daily de-trended values of Z700 height. Given the model high spatial resolution (about 30 km around the Mediterranean), a bilinear interpolation scheme is first applied to convert the dataset into a regular grid of $\mathring{1}$ by $\mathring{1}$ in longitude and latitude.

Given the availability of the ISCCP, E-OBS and ERA40 datasets, we have chosen the December 1983–February 2000 period (17 winter seasons) as the common period for evaluating the twentieth century simulation of the LMDz model. In order to evaluate the effect of increased GHG concentration and aerosols given by the SRES A1B during the period 2000–2050, we have calculated differences between the reference periods 1961–1990 and 2021–2050. As mentioned before, the ERA40 clusters were calculated for the winter period December 1961–February 2002, and the relative percentage of clusters calculated for the two periods of interest: evaluation: 1983–2000; twentieth century: 1961–1990. Summary of the results are given in Table 1.

4 Results

General features of the winter-time climatology over the Mediterranean region are first outlined (Sect. 4.1). Then, the results for the observationally based and LMDz modelling based (Sect. 4.2) weather regime are analysed and discussed. Followed by a short discussion of clouds in LMDz (Sect. 4.3). In Sect. 4.4 we evaluate and analyse the projected changes in precipitation and temperature for the last 30 years of the simulation (2021–2050) in the context of changing winter weather regimes. The winter season is referred to by the year of the first month, i.e., winter 1999 corresponds to December 1999, and January and February 2000.

4.1 Climatological winter conditions in the Mediterranean basin

Figure 1 shows the winter-time climatology (1983–1999) of total cloud cover, precipitation, mean surface temperatures and sea surface temperatures, from the ISCCP and E-OBS datasets (left panels), and the differences between model and observational dataset (right panels), in absolute terms for cloud cover and temperatures, and as percentage for precipitation.

The ISCCP winter total cloud cover (Fig. 1a) shows a latitudinal gradient, with highest values over the Atlantic Ocean and Black Sea (up to 80–90 %) and lowest values over Northern Africa (30–50 %). Cloud cover over the Mediterranean Sea varies between 50 and 70 %, whereas higher values (70–80 %) are found over the European continent. The LMDz model underestimates the cloud cover over the whole domain (Fig. 1b), but reproduces reasonably well the latitudinal gradient. Over the Mediterranean basin LMDz underestimates the ISCCP cloud cover by 10–30 %, with smaller differences (10–20 %) over western and south-western Europe and higher (20–40 %) over south-eastern Europe and North Africa.

The winter surface temperatures over the domain are warmest over northern Africa and the Iberian Peninsula, and get gradually colder towards the north and eastern part of the domain. In general, the LMDz mean surface temperatures are in reasonable agreement with those from E-Obs dataset, though there is an overall cold bias (Fig. 1d). This bias is smallest over France (less than 0.5 °C), is 0.5–2 °C over the Iberian Peninsula, Northern Africa, central and north-eastern Europe, and between 2 and 3 °C in some high-altitude areas like the Alps or the Italian and western Balkan's mountain ranges.

The Sea Surface Temperatures (SSTs) show a latitudinal gradient from south to north, with values between 13 and 19 over the Mediterranean Sea (Fig. 1e). LMDz has a cold SST bias with values between 0.5 and 2.5 °C (Fig. 1f). This is due to a cold SST bias from the global model (up to 4 °C over the Atlantic sector, not shown), which is reduced in the regional coupled system. The same coupled model, when driven by more realistic large-scale boundary conditions, shows much improved temperature (L'Hévéder et al. 2012). The larger cold biases in surface temperatures in the eastern part of the domain are probably influenced by this cold Mediterranean SST bias. The cold SST bias could also be responsible for the lower cloud cover simulated by the model over the Mediterranean Sea.

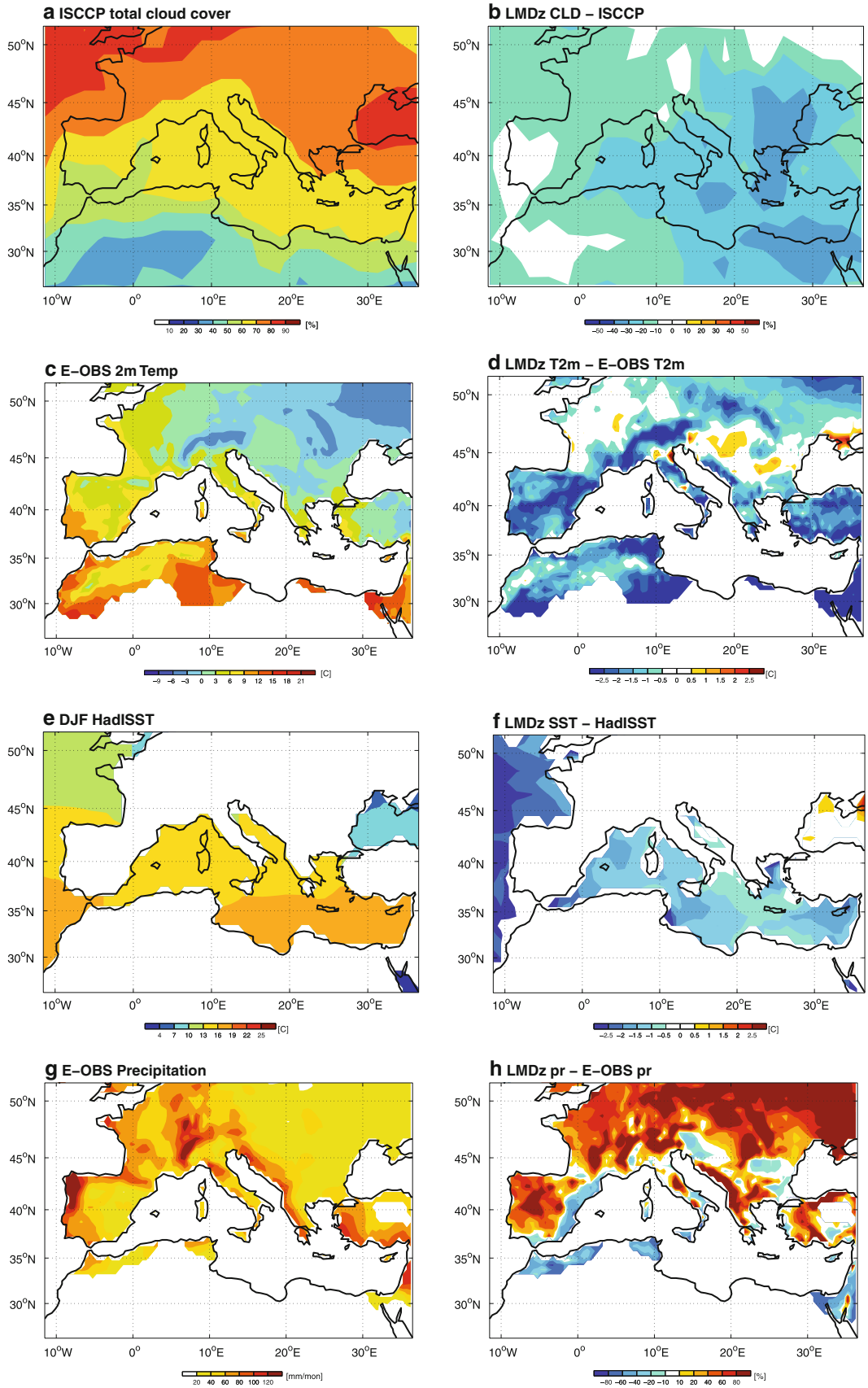
a ISCCP total cloud cover
b LMDz CLD – ISCCP
c E–OBS 2m Temp
d LMDz T2m – E–OBS T2m
e DJF HadISST
f LMDz SST – HadISST
g E–OBS Precipitation
h LMDz pr – E–OBS pr
50°N
45°N
40°N
35°N
30°N
10°W
0°
10°E
20°E
30°E
[%]
[C]
[mm/mon]

Table 1 Frequency of occurrence of ERA40- and LMDZ-based four main winter weather regimes (cyclonic, anticyclonic, meridional and zonal) over the Mediterranean basin (in % of total winter days)

Period	Cyclonic	Anticyclonic	Meridional	Zonal
ERA40: 1983–1999	22.0	28.0	25.2	24.8
ERA40: 1961–1990	23.0	25.5	25.3	26.1
LMDz eval: 1983–1999	21.9 (R = 0.94)	20.6 (R = 0.97)	28.4 (R = 0.95)	29.1 (R = 0.98)
LMDz 20C: 1961–1990	22.1	24.9	25.9	27.1
LMDz 21C: 2021–2050	20.1	30.0	25.4	24.5

During winter, significant precipitation (20–140 mm/month) falls over land throughout the entire study region (Fig. 1e). The highest values (both observed and simulated) occur in western Europe, along the Atlantic coasts, and in the western parts of the major Mediterranean peninsulas (Iberian, Italian, Balkan and Anatolian). Precipitation is enhanced by the orographic relief with high mountains, like the Alps, Pyrenees in France and Apennines in Italy. The model reproduces the overall spatial pattern of precipitation, but overestimates it over most European continental areas, especially mountainous ones at the west coasts (by about 80 %, Fig. 1f). As a consequence it underestimates the east coasts precipitation as well as that at the northern African coast. The topographic enhancement of precipitation in regional models is a well known problem, found in different RCM and regions (e.g., Coppola et al. 2010; Rojas 2006).

In summary, the LMDz model reproduces the spatial pattern of the satellite- and surface-based climatological winter time cloud cover, surface temperatures and precipitation, with the following biases: it underestimates cloud cover, it has a cold temperature bias, while it overestimates precipitation (mainly orographic).

4.2 Climatologies of winter weather regimes over the Mediterranean basin from ERA40, observational datasets and LMDz

We applied the clustering algorithm, described in Sect. 3, to both ERA40 and LMDz Z700 (both for the period 1960–1999) to determine the four regimes controlling wintertime weather over the Mediterranean, percentage of occurrence of each regime is calculated for the period 1983–1999 only. Figure 2a–d displays the four weather regimes derived from ERA40 analysis and Fig. 2e–h the regimes from LMDz model. Z700 anomalies are shown with colour shading whereas the composites of each cluster (Z700 values) are given as black contours. Between 85 and 80 % of the individual events that fall into one particular cluster last for longer than 2 days, hence we term them "regime".

Based on the configuration of ERA40 large-scale Z700 and their anomalies, the four clusters have been termed as: (1) Cyclonic regime (least frequent regime: 22 % occurrence), (2) Anticyclonic regime (most frequent regime: 28 %), (3) Meridional regime (25.2 % occurrence) and (4) Zonal regime (24.8 % occurrence).

The main four winter clusters from LMDz (Fig. 2e–h) closely match the ones obtained from ERA40 (Fig. 2a–d), especially in terms of anomalies, with some differences in the relative frequency of occurrence (Table 1). A correlation analysis indicates that the ERA40 and LMDz clusters are indeed highly correlated (R = 0.94–0.98, shown in table 1). Table 1 summarises the relative frequency of occurrence of all ERA40 and LMDz regimes, including those of LMDz simulations for the twentieth and twenty-first centuries. These results indicate the ability of the LMDz model to reproduce the weather regimes prevailing over the Mediterranean during winter.

The patterns of atmospheric and surface variables, associated with each of these regimes, specifically, the fields of cloud cover, precipitation, maximum and minimum surface air temperatures (T2 m) and surface downward solar and thermal radiation where calculates and are described below. To ease the lecture, we have provided a schematic diagram summarizing each ERA40 regime. The full ERA40 figures can be found as online supplementary material. For each regime we first describe the ERA40/Observational fields and then the LMDz composites.

4.2.1 Cyclonic regime

The Cyclonic regime is characterized by a strong negative geopotential anomaly over France (brown contours in Fig. 3a). This circulation anomaly induces higher-than-normal cloudiness over the Mediterranean basin west of the Balkans and in western North Africa (>20 %). Positive precipitation anomalies are associated with higher cloud clover. Whereas lower cloudiness prevails over the south-

◀ **Fig. 1** DJF climatological mean fields for evaluation period:1983–1999. **a** ISCCP cloud cover, **b** ISCCP cloud cover—LMDz cloud cover, **c** E-OBS 2 m mean temperature, **d** LMDz—E-OBS 2 m mean temperature, **e** HadISST Sea Surface Temperatures (SSTs), **f** LMDz—HadISST, **g** E-OBS precipitation, **h** E-OBS—LMDz precipitation (percentage)

eastern Mediterranean Sea and in central and eastern North Africa. Consequently, there are negative downward surface solar radiation anomalies over areas with positive cloud cover anomalies (up to −20 %). Negative maximum and minimum temperature anomalies are seen over Central and Northern Europe, and positive anomalies to the south, over the North African coasts and over the Balkans and Anatolian Peninsula.

Differences in maximum and minimum temperatures are not included in the schematic. Over western North Africa (northern Algeria and Morocco) and over the south-eastern Iberian Peninsula positive minimum T2 m anomalies prevail by the presence of enhanced cloud amounts. Clouds trap part of the emitted thermal radiation from the surface during night and re-emit down to surface, in line with the positive anomalies of downward surface thermal radiation over these regions (by about 10 %, purple arrows). Thus, in this region, enhanced cloudiness results in reduced daily temperature amplitude. On the other hand, over the Balkans and the Anatolian peninsulas, the positive T2 m anomalies are explained by the advection of warmer air from North Africa driven by the cyclonic circulation that affects both minimum and maximum T2 m (between 2 and 3 °C).

Although this regime is the least frequent one, its precipitation has a large contribution to the total seasonal precipitation. For example the Iberian Peninsula receives 35–45 % of the total seasonal precipitation during these events, Alps and Italy between 50 and 60 % and the rest of south-eastern Europe between 40 and 60 %.

4.2.1.1 LMDz cyclonic regime The LMDz cyclonic regime has similar features of Z700 and associated anomalies to the ERA40 regime, with a less pronounced trough around 5–10°E (see Fig. 2). Similarly to the ERA40 regime, the LMDz is characterised by positive total cloud cover anomalies over almost the whole Mediterranean region, with values up to 50 % over the Italian, Balkans and Anatolian peninsulas (see Fig. 4), but is more extended than the ERA40. Significant positive precipitation anomalies (Fig. 4b) appear over most of the region, with negative precipitation anomalies in the northernmost part of the domain, (similarly with the ERA40 regime) and over north-eastern Africa, which is not covered by the observational dataset.

As in the ERA40 cyclonic regime, the surface downward solar (Fig. 4e) and thermal (Fig. 4f) radiation anomalies are strongly related to those of cloud cover and T2 m. The LMDz solar radiation anomalies at surface are enhanced above regions with high altitude (up to 50 %) reflecting thus topographic features in the LMDz model. Temperature anomalies are driven by a combination of circulation advection and cloud cover, and are overall well reproduced by the model (Fig 4c, d). Differences in the north-eastern part of the domain, can be attributed to the deeper cyclonic anomaly and stronger warm south advection in the model. Remarkably, the warmer-night/colder-days feature that is observed over the Iberian Peninsula is well reproduced by the model, albeit smaller minimum T2 m anomalies.

Fig. 2 Climatological (1983–1999) four weather regimes prevailing over the Mediterranean during winter (December–January–February) in terms of geopotential height at 700 hPa (Z700 contours in km). *Coloured areas* represent the Z700 anomalies (in m) with respect to the climatological fields. Results are given from the application of cluster analysis to Z700 fields from: ERA40 (**a**, **b**, **c**, **d**) and LMDz model (**e**, **f**, **g**, **h**) ▶

One important difference with the ERA40 regime is that the model does not reproduce the positive minimum temperature anomalies over Morocco/Algeria, though it simulates the negative maximum T2 m anomalies. Positive minimum T2 m anomalies can be explained by night-time heat trapping by clouds. The fact that the model has higher than normal cloud cover in this region (Fig. 4a) but does not reproduce heat trapping might be due to the vertical distribution of clouds by the model. In the model the enhanced cloudiness is due to low-level clouds, and not to high-level ones, which are most efficient in trapping heat. On the contrary, negative high-level cloud anomalies are simulated by the model (not shown).

4.2.2 Anticyclonic regime

This regime is characterized by a pronounced north–east ridge extending over southern France and Germany, with strong positive geopotential anomalies centred over southern France, spreading out down to the Mediterranean basin (Fig. 3b). Lower than normal cloud cover is found over the whole region between 25 and 50°N, with more clouds over north-eastern African regions (Libya and Egypt). Very dry conditions occur during this regime, with the strongest negative precipitation anomalies (up to −80 %) over Italy, the Alps and the western Greek and Anatolian peninsulas, i.e. where the largest negative cloud cover anomalies occur. Precipitation amounts associated with this regime contribute very little (less than 15 %) to the total seasonal precipitation over most parts of the domain.

This anticyclonic regime induces positive anomalies of maximum T2 m over most of the domain (Fig. 5d), except the regions surrounding the eastern basin, and of minimum T2 m over all European areas north of 40̊N. The negative maximum and minimum T2 m anomalies over Greece and Turkey are influenced by the circulation patterns found at the edge of positive Z700 anomalies (Fig. 2b). The fields of regional surface downward solar (Fig. 5e) and thermal

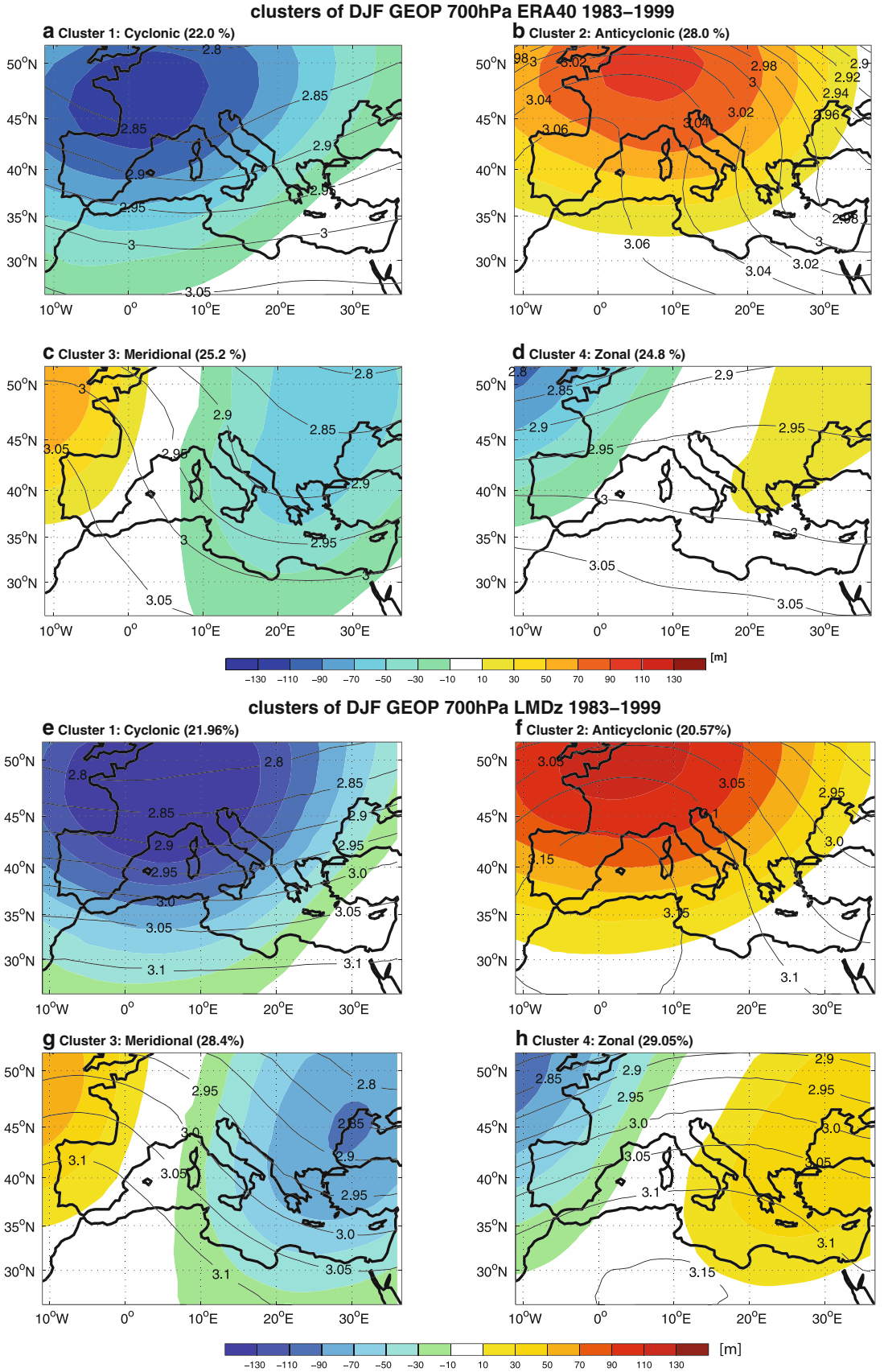
clusters of DJF GEOP 700hPa ERA40 1983–1999
a Cluster 1: Cyclonic (22.0 %)
b Cluster 2: Anticyclonic (28.0 %)
c Cluster 3: Meridional (25.2 %)
d Cluster 4: Zonal (24.8 %)
clusters of DJF GEOP 700hPa LMDz 1983–1999
e Cluster 1: Cyclonic (21.96%)
f Cluster 2: Anticyclonic (20.57%)
g Cluster 3: Meridional (28.4%)
h Cluster 4: Zonal (29.05%)
50°N
45°N
40°N
35°N
30°N
10°W
0°
10°E
20°E
30°E
[m]
−130 −110 −90 −70 −50 −30 −10 10 30 50 70 90 110 130

(Fig. 5f) anomalies are generally in line with the patterns of cloud cover and T2 m: positive/negative anomalies of downward solar/thermal radiation all over southern Europe.

4.2.2.1 LMDz anticyclonic regime As in the observations, this regime is the most frequent weather regime during the winter season in the LMDz model, occurring almost 28 % of the days (compared well to the 28 % in ERA40, see Fig. 6). The positive geopotential anomalies centred over France, are somewhat stronger in the model compared to ERA40. Similarly to the ERA40 regime, negative total cloud cover anomalies (Fig. 6a) are found over most of the domain, with important negative precipitation anomalies (up to 80 %) over Italy, Alps, western Balkans and southern Iberian Peninsula, except over eastern northern Africa and off its coastal areas (Fig. 6b). In this region, lying outside the E-OBS database domain, the model indicates important positive precipitation anomalies.

In the model, the regime is further characterized by positive (negative) solar (thermal) downward radiation anomalies (Fig. 6e, f) at surface, resembling the cloud cover pattern. These stronger radiation anomalies are enhanced over topographic features, and are not seen in the ERA40 regime. Both maximum and minimum T2 m anomalies (Fig. 6c, d) show a distinct north-west/south-east positive/negative dipole structure that is more pronounced than in the ERA40 regime, but overall very similar. According to the model anticyclonic regime, negative T2 m anomalies exist over the Mediterranean basin, with maximum values in its eastern part.

4.2.3 Meridional regime

This regime is characterized by a trough extending over the Balkans with its axis reaching north-eastern Africa, and brings into the Mediterranean air from north-western Europe and the Atlantic Ocean. Negative Z700 anomalies persist over the eastern half part of the region (east of 10̊E) against positive Z700 anomalies over the Iberian Peninsula and most of France (Fig. 3c).

Cloud cover is lower than the climatological wintertime mean over the western Mediterranean whereas it is slightly higher in the central and eastern basins. Associated to this cloudiness pattern, negative precipitation anomalies are found over the Iberian Peninsula, France and Italy, and positive precipitation anomalies over northern Europe, the Balkans and Anatolian peninsulas. The total precipitation of this

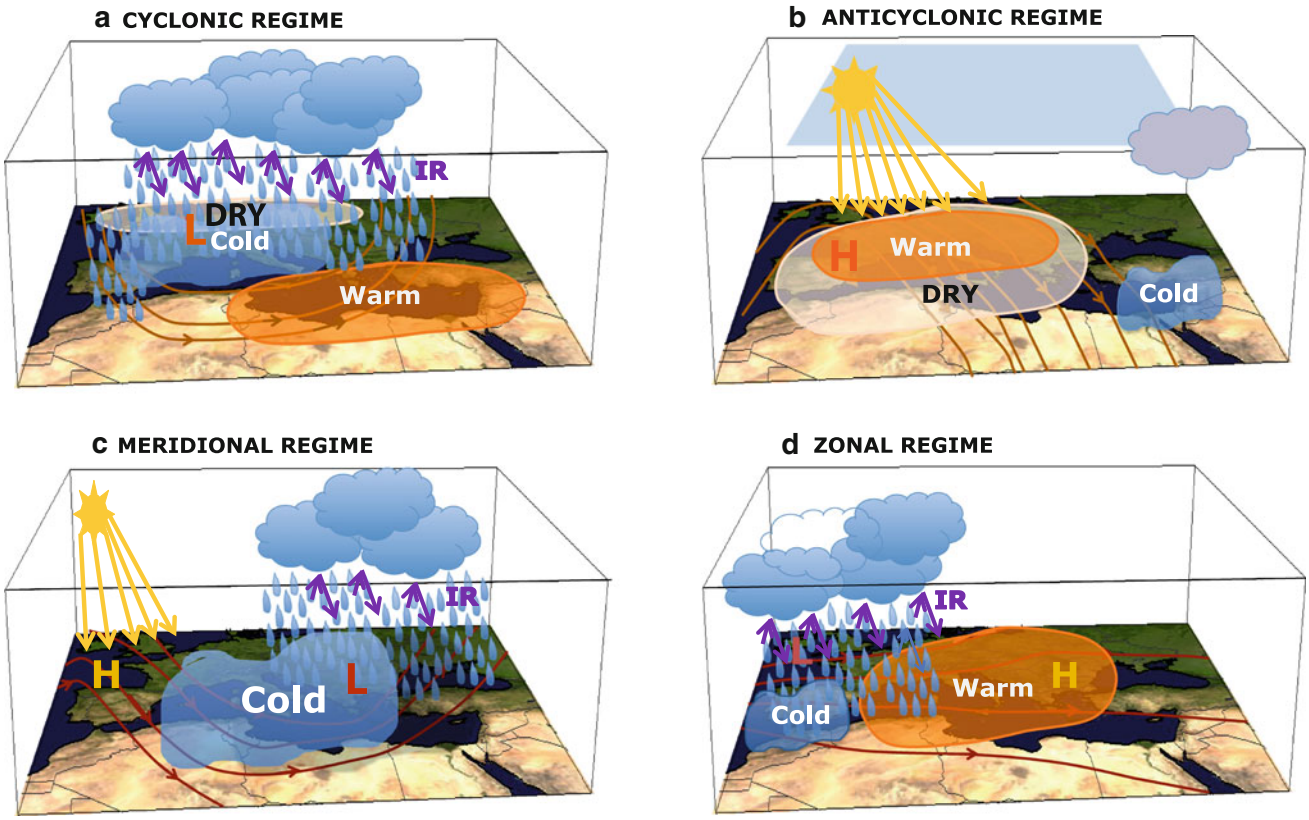

Fig. 3 Schematics of the four ERA40 winter regimes, including anomalies of Z700, cloud cover, precipitation surface temperatures and infrared radiation. **a** cyclonic regime, **b** anticyclonic regime, **c** meridional regime, **d** zonal regime

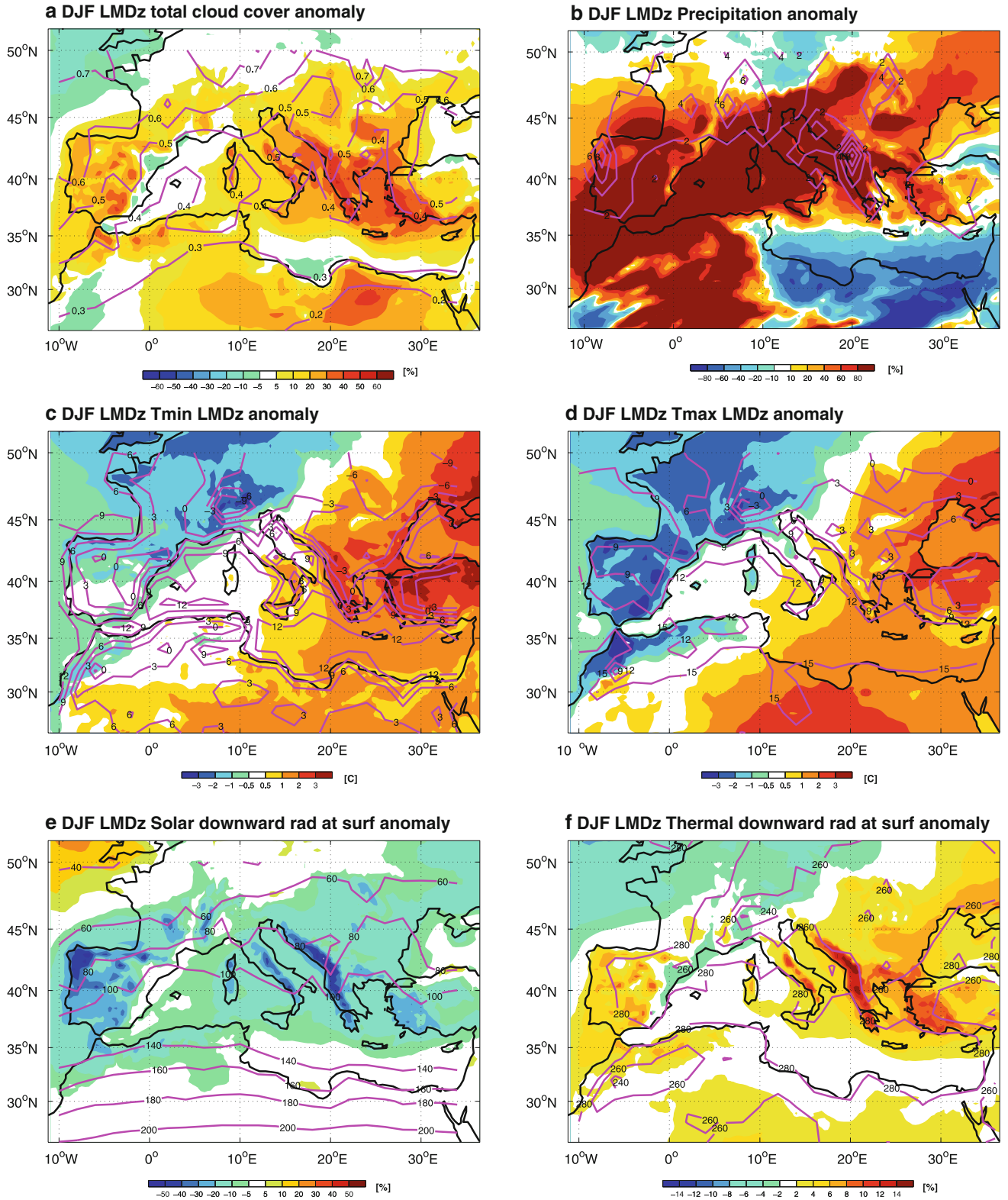

Fig. 4 Geographical distribution of the anomalies of winter surface and atmospheric conditions over the Mediterranean region for LMDz cyclonic weather regime (21.9 %) **a** total cloud cover, **b** precipitation, **c** min temperature, **d** max temperature, **e** solar downward radiation at surface, **f** solar upward radiation at surface **g** thermal downward radiation at surface, **g** thermal downward radiation anomaly at surface, **h** thermal upward radiation at surface

regime contributes to up to 50 % of the total winter precipitation (maximum contributions over the Alps and Turkey).

The patterns of surface downward solar and thermal radiation anomalies are fully in line with those of cloudiness, with positive/negative solar/thermal radiation anomalies in the western Mediterranean basin and negative/positive anomalies, respectively, in the eastern part of the basin. During this regime, most of central part of the domain is colder than normal, except over the Iberian and Anatolian peninsulas that exhibit positive anomalies of maximum and minimum T2 m, respectively. These anomalies increase the daily temperature amplitude over the Iberian Peninsula (similarly to the cyclonic regime) and decrease the daily temperature amplitude over the Anatolian Peninsula.

4.2.3.1 LMDz meridional regime The meridional regime (Fig. 2g) occurs 25.2 % of the winter days in the LMDz model, the same as in the ERA40 data, and resembles closely the Z700 isolines and anomalies, albeit a further eastward shifted centre, and deeper geopotential anomalies. As a consequence of the further eastward displaced Z700 anomalies, the negative/positive cloud cover anomaly (Fig. 8a) over the western/eastern part of the Mediterranean basin is extended more eastward than in the ISCCP data. Hence the precipitation anomaly pattern is also displaced further eastward. However, the main difference with the ERA40 regime is an important enhancement of the negative temperature anomalies (model anomalies are up to 1 °C colder, Fig. 8c, d), and the enhanced model solar and thermal downward radiation anomalies (up to 10 and 5 % respectively, Fig. 8e, f).

The pattern and amplitude of the cold temperature anomalies in this regime could be explained by the stronger temperature advection induced by the circulation pattern of this regime. Over the Iberian Peninsula the positive maximum temperature seen in the observations are only marginally reproduced in the model (see Fig. 8d, 0.5 in the model versus 1 °C observed anomalies). Therefore the model underestimates the enhanced daily temperature range seen in the observations.

4.2.4 Zonal regime

This regime brings humid air from the Atlantic to the Mediterranean (Fig. 3d), and shows in most variables the opposite pattern than the meridional regime. When it occurs, negative Z700 anomalies prevail over western part of the domain and positive on the eastern side. More than average cloudiness occurs in the western Mediterranean basin through to the Italian and western Balkans peninsulas, together with precipitation (Fig. 3d). Slightly less cloudiness appears over the eastern Mediterranean basin, with negative precipitation anomalies. The positive precipitation anomalies of this regime contribute 30–50 % of the total winter precipitation in France and the Iberian Peninsula.

The anomalies of surface radiation during this regime are clearly smaller than those of all other weather regimes. There are negative solar and positive thermal downward radiation anomalies at surface (up to 20 and 10 %, respectively), in a spatial pattern resembling the cloud cover anomalies. The temperature anomalies of this regime are also more moderate than the other three. They are positive throughout the basin, except for negative maximum T2 m anomalies over the Iberian Peninsula, which together with positive minimum T2 m anomalies in this region reduce the daily temperature range.

4.2.4.1 LMDz zonal regime The zonal regime occurs 29 % of the winter days in the LMDz model (see Fig. 2h), and compared to the corresponding ERA40 regime (Fig. 2d), has a less zonal geopotential pattern (black contours). The anomaly field (shaded contours) does resemble well the ERA40 regime (see Fig. 2d) though with slightly more expanded positive anomalies in the eastern part of the domain. The total cloud cover anomaly (Fig. 7a) is mostly positive (up to 50 %), and spreads further to the east than in the ERA40 regime, accordingly important positive precipitation anomalies (Fig. 7b) are found over northern Africa, the Iberian Peninsula, France and the Alps, similar to the ERA40 regime.

As for the meridional regime, the temperature and radiation anomalies (Fig. 7c–f) of the zonal regime are larger and geographically more expanded in the LMDz model than in the ERA40 dataset. The temperature anomalies are positive with values up to 3 °C (both minimum and maximum temperatures, Fig. 7c, d), especially over Italy and the Balkans. Largest radiation anomalies (Fig. 7e, f) are found over these same regions, negative solar downward anomalies (up to −20 %) and positive thermal downward radiation (up to 10 %). The model also reproduces the observed decreased daily temperature amplitude over the Iberian Peninsula during this type of events.

4.3 LMDz cloud level and temperature anomalies

The LMDz model enables the investigation of some additional characteristics of the identified weather regimes, for example how these regimes affect the low, mid and high level clouds, in addition to their impact on the total cloud cover fields discussed above. This is important given the different role of each cloud type for the shortwave and longwave radiation budgets, and hence the regional climate. To this aim, the composite of the cloud fields for the 4 model WRs have been calculated (not shown).

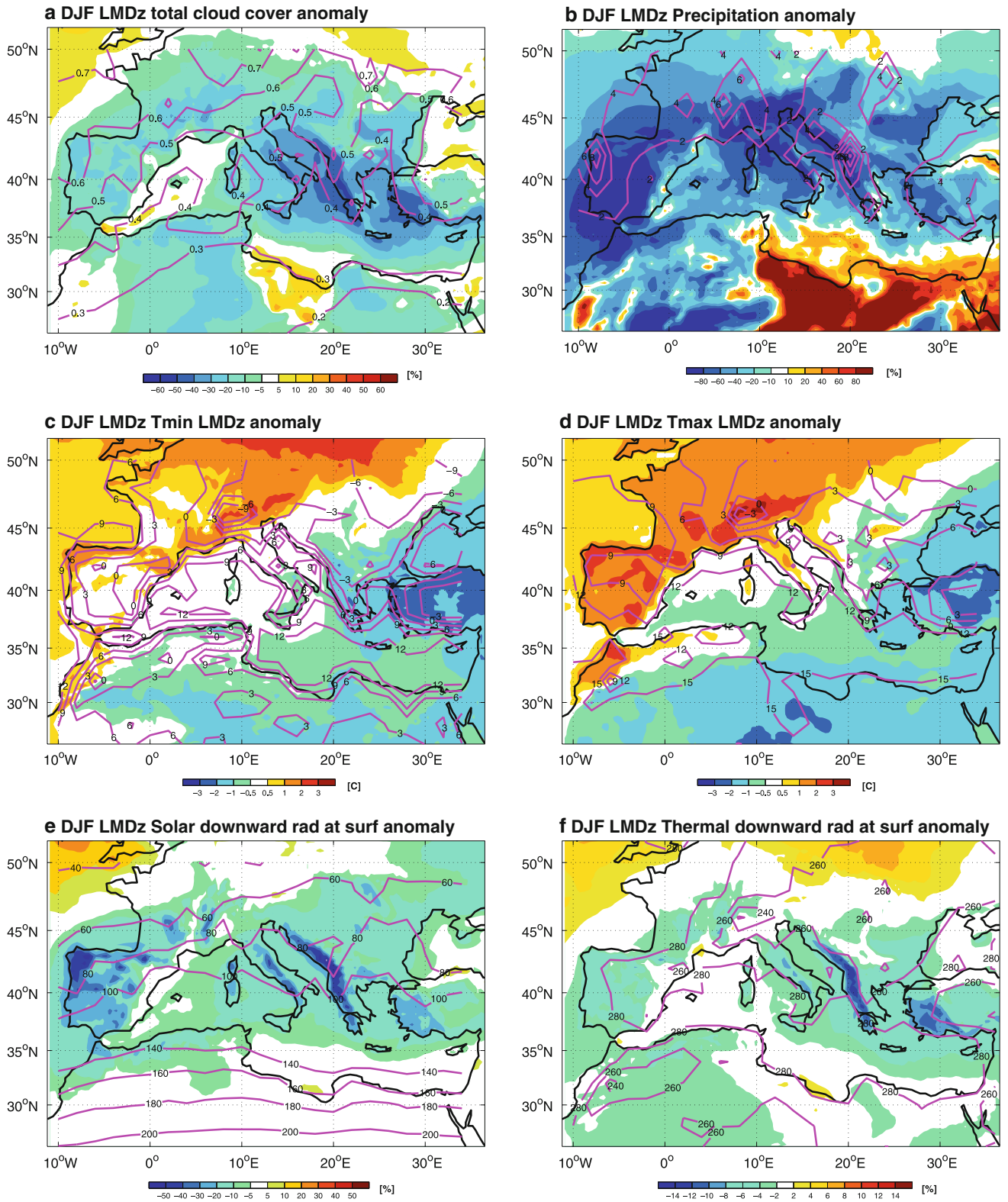

Fig. 5 Same as Fig. 4, but for the LMDz anticyclonic weather regime (20.6 %)

LMDz has 4 cloud variables, low, mid and high level clouds as well as total cloud cover, which is a column-integrated cloud cover with assumption of random overlapping. Low-level clouds correspond to cloud cover in the lower levels of the model, up to 500 hPa. Mid-level clouds are found between 500 and 300 hPa. High-level

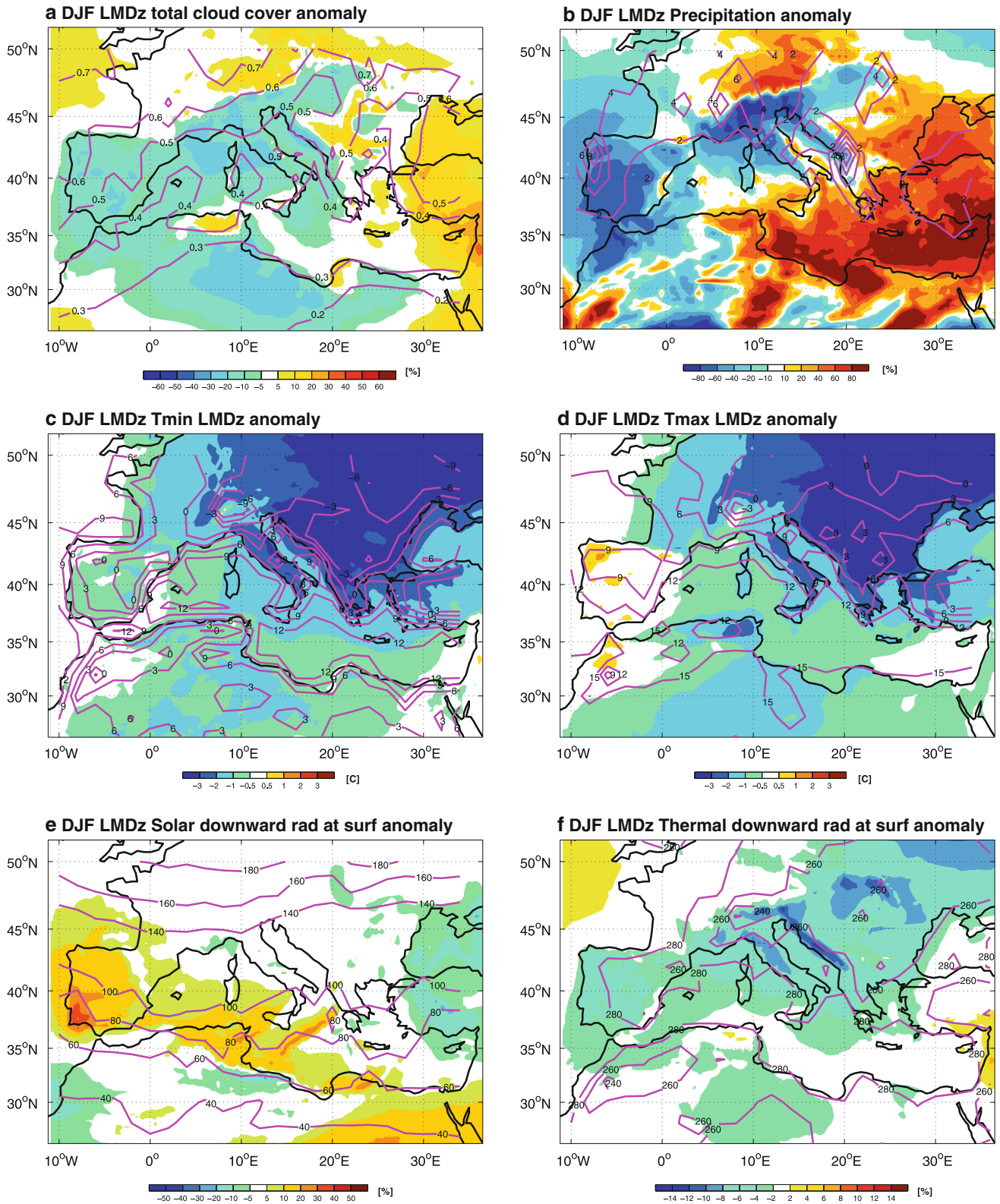

Fig. 6 Same as Fig. 4, but for the LMDz meridional weather regime (28.4 %)

clouds are above 300 hPa and correspond mainly to cirrus clouds. Convective clouds are separated at each level, but are mainly found at low and mid-level in the model.

In all four regimes, positive precipitation anomalies are mainly correlated with the mid-level clouds, and to a lesser degree with low-level clouds. Solar downward radiation anomalies are best anti-correlated to the total cloud anomaly, whereas the thermal downward radiation is strongly correlated to high-level clouds, which mainly represent cirrus clouds in the model. As has been discussed already in the regime characterisation, maximum and minimum temperatures are determined both by temperature advection induced by the circulation anomalies, and by cloud fields. Consideration of different levels of clouds shows that the pattern of high-level clouds shapes the temperature anomalies in the model. Temperature discrepancies found between the ERA40 and LMDz WRs (as discussed for the cyclonic regime over northern Africa for example), can be explained by the type (level) of clouds simulated by the model.

4.4 Mediterranean climate change projection

The last 30 years of simulation, 2021–2050, show projected climate changes following the SRES A1B scenario. Figure 8 shows the cloud cover, 2 m temperatures, SSTs and precipitation differences between the periods 2021–2050 and 1961–1990. Seven regions used to calculate regional precipitation differences are also indicated.

The LMDz simulation indicates that a general decrease of cloud cover (Fig. 8a) is foreseen for Europe and the Mediterranean Sea, by up to about 5–10 % in most areas, reaching −15 % above the eastern Mediterranean basin, including Greece and Turkey. A general warming over the study region is also projected, with an increasing gradient from the south-west to north-east (Fig. 8b). Smallest warming is projected in most of northern Africa and Portugal (up to 1.5 °C). Warming up to 2 °C is foreseen over the Iberian Peninsula, France, and the Mediterranean Sea, against stronger warming moving eastwards into the European continent, reaching up to 4 °C in the north-eastern part of the domain. This warming is in accordance with previous studies (Déqué et al. 2012 and references therein) and IPCC AR4 projections for the region (Christensen et al. 2007), and is similar to the projected warming of the driving model. The SSTs differences are somewhat smaller than the 2 m temperatures in the model, especially near the coasts. Finally, the model simulation predicts a 5–20 % decrease in precipitation in the Mediterranean region (up to 42°N, Fig. 8d), and unchanging or positive precipitation changes north of 45°N. The spatial pattern of the precipitation changes for the twenty-first century is related to the total cloud cover pattern. This accordance is even stronger between low and mid-level clouds and precipitation changes (not shown).

In order to analyse the changes shown in Fig. 8 in terms of weather regimes, the cluster analysis was applied to the Z700 fields of the LMDz twenty-first century's simulation. The analysis yielded the same four weather regimes that had been identified for the recent decades. The comparison between the weather regimes of the twentieth and twenty-first centuries was however calculated from the cluster analysis of the complete (1961–2050) period, and reveals changes in their relative frequency of occurrence (see Table 1). More specifically, the cyclonic and zonal regimes become less frequent (decreasing from 27 to 24.5 % and from 22 to 20 % respectively), and the anticyclonic regime becomes more frequent (increasing from 25 to 30 %). There is no significant change in the frequency of the meridional regime. The cyclonic and anticyclonic regime also differ somewhat from their twentieth century counterpart in that the Z700 anomalies are larger, i.e., deeper low over France for the cyclonic regime and higher high in the anticyclonic regime. A consequence of this difference is that for example, the relative contribution of rainfall to the total winter total of the cyclonic regime is larger in some regions as the Alps during the twenty-first century compared to the twentieth century.

The projected changes in relative frequency of the four weather clusters can partly explain the simulated changes of temperature and precipitation shown in Fig. 8. For example, increasing frequency of the anticyclonic cluster leads to more days with dry and warm conditions over most of the Mediterranean Basin and western Europe respectively. Whereas decreasing frequency of the cyclonic WR contributes to the decreasing precipitation over most of the region and less days with negative temperature anomalies in the western part of the region (Fig. 4a, c, d), i.e. warmer conditions. Less frequent zonal cluster also contributes to less precipitation over the Iberian Peninsula and France and the Alps. All changes of WRs' frequency are statistically significant (t test) at the 95 % confidence level.

In order to further quantify the contribution of the change in relative occurrence of each WR to the total precipitation change, we have defined 7 regions to take regional averages. The regions are indicated in all panels in Fig. 8. In Fig. 8d, we see that over Iberian Peninsula (IBS), Western and North Eastern North Africa (WNA, ENA) and Balkans (BAL) regions there is a precipitation decrease projected for the twenty-first century. The other regions show no significant precipitation decrease (around 5 %). This precipitation change in all 7 regions is shown in the lower bars in Fig. 9. For example for IBE our simulation projects a 15 % decrease in the winter precipitation, and over Western and Eastern North Africa (WNA and ENF respectively) the projected decrease is about 20 and 10 %

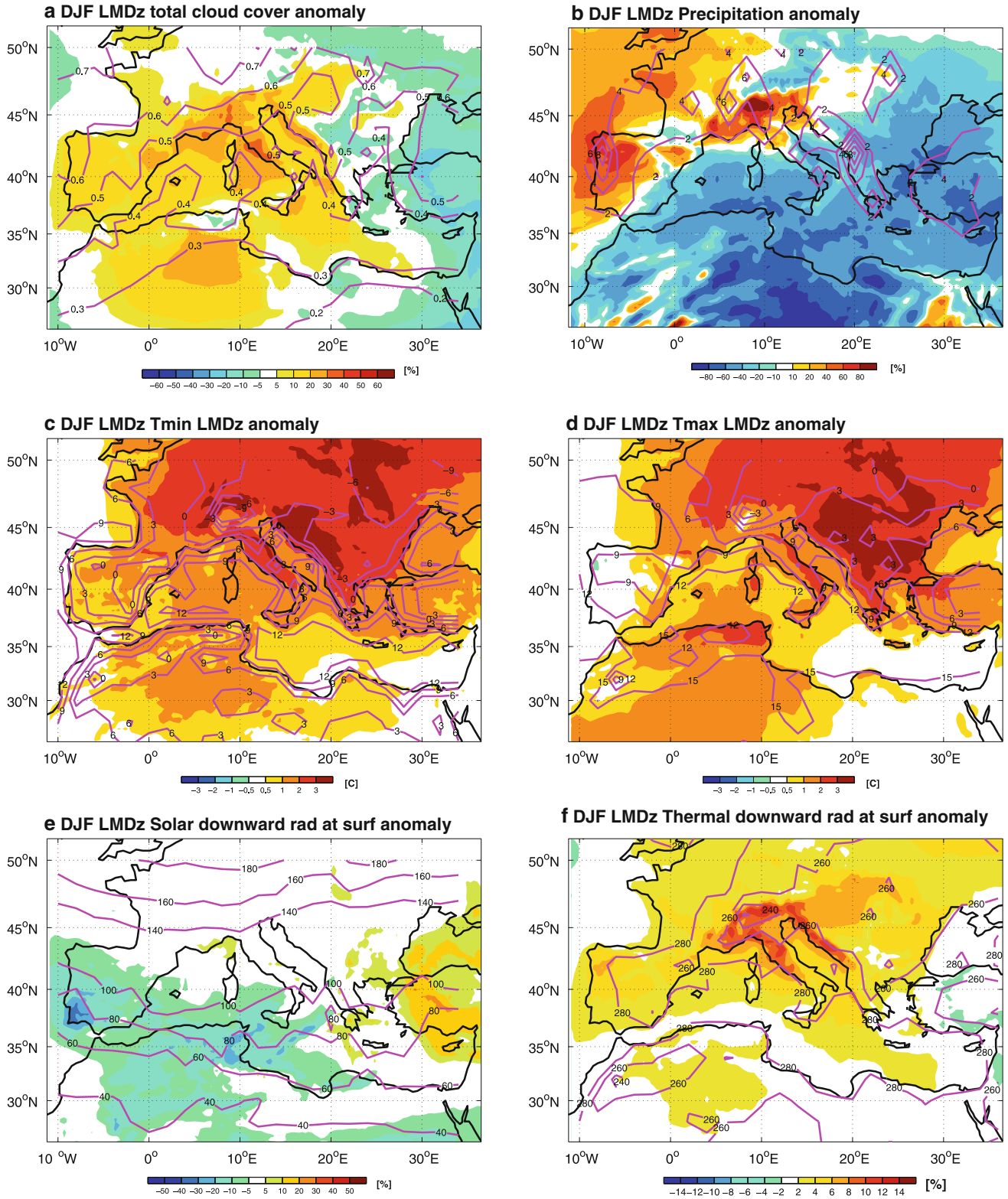

Fig. 7 Same as Fig. 4, but for the LMDz zonal weather regime (29.1 %)

respectively. Bars in the upper part in Fig. 9 show the percentage of the total change that can be attributed to each of the 4 clusters. For example, over the Iberian Peninsula, 50 % of the decrease comes from a change in the cyclonic clusters (that decreases in frequency from 22 to 20 %), and between 10 and 15 % of the three other clusters. In the case

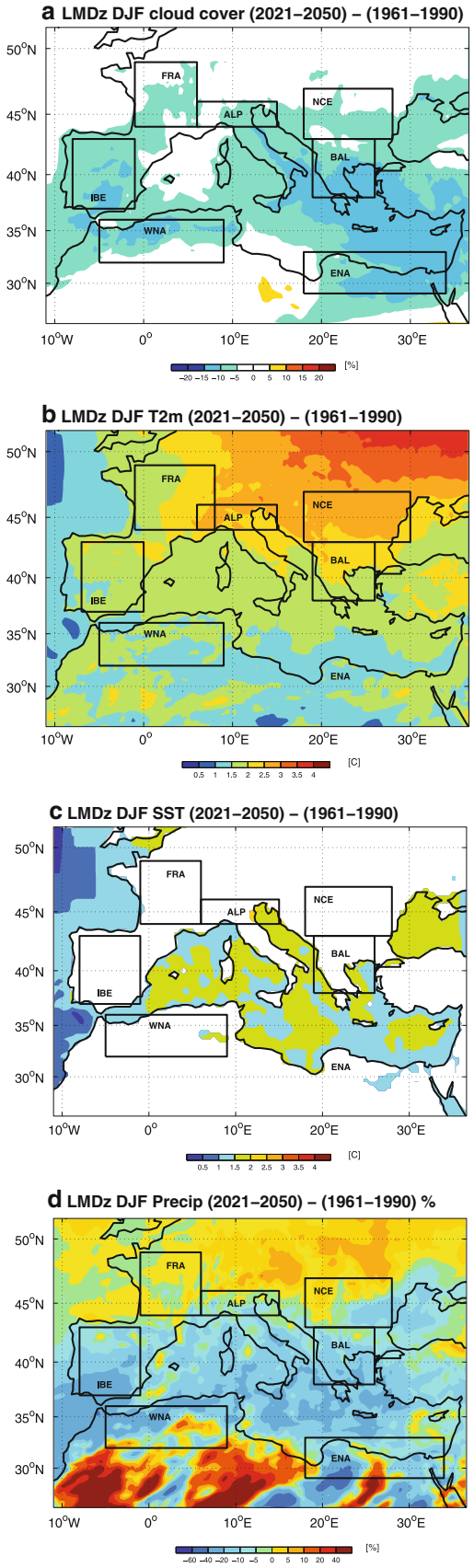

◀ **Fig. 8** Climate change projections for the Mediterranean region. **a** percentage Cloud cover differences (in %), **b** Absolute temperature difference (in C), **c** absolute SST differences, **d** precipitation % difference between the twenty-first and twentieth century. Also indicated in each panels are the 7 regions for which regional precipitation changes are calculated (and shown in Fig. 9). Regions are: Iberian Peninsula (IBE), France (FRA), Western North Africa (WNA), Eastern North Africa (ENA), Northern Central Europe (NCE), Balkans (BAL), and Alps (ALP)

of the region FRA there is no net change is precipitation, but the cyclonic and anticyclonic clusters contribute to an increase in precipitation (negative bars) and the meridional and zonal clusters to a decrease. Although there is a small decrease in the frequency of occurrence of the cyclonic type of events in the future, for the Alpean region, the amount of precipitation that falls during these events represent a larger fraction of the total winter precipitation than during the 20C.

A final aspect of the WRs that is analysed is the continuity or duration of each regime and the associated climate variables and the projected change in the twenty-first century. To study this characteristic we have defined the so-called "weather regime (WR) events", which are consecutive days characterized by the occurrence of one of the four WRs in the region. Figure 10 shows the distribution of the WR events of each regime as a function of their duration (1–3, 4–6, 7–10 days, etc.). The results are given separately for the two periods of the model simulations, i.e. for the twentieth century (green bars) and for the climate change projection of the twenty-first century (brown bars), and for the ERA40 as reference (blue bars). Figure 10 also shows the median (red line) and the 25th and 75th percentiles (blue box edges; the whiskers extend to the most extreme data points, and red crosses represent outliers) of the event length for each regime in the twentieth and in the twenty-first centuries. On average, the four WRs last between 3 and 5 days, with long duration events lasting up to 10–15 days (75th percentile). Compared to the duration of the ERA40 regimes, the LMDz reproduces very well all median regime lengths, except the zonal regime, which is generally is shorter in ERA40.

Analysing the results for the twentieth century reveals differences between the four LMDz WRs in relation to their continuity and length. The cyclonic and anticyclonic WRs are more persistent, with 75th percentile of events lasting up to 7–8 days and maximum length up to 25 days, whereas the meridional and zonal regimes are generally shorter, with 75th percentile of 5 days and maximum length of up to 15 days. The mean duration of the WRs events is 4, 5, 3.5 and 4 days, for the cyclonic, anticyclonic, meridional and zonal regimes, respectively. The mean duration of the same regimes in the twenty-first

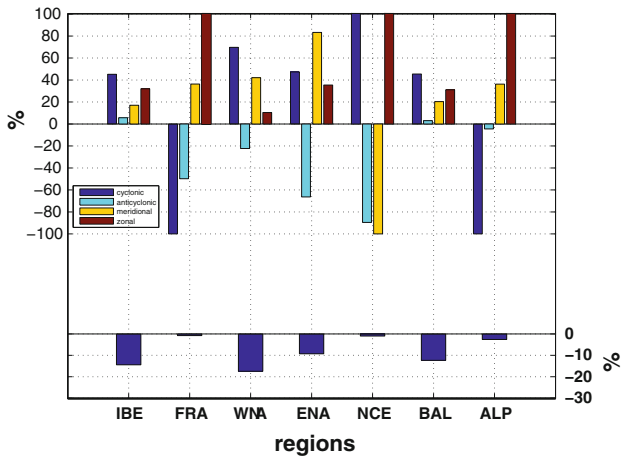

Fig. 9 Regional precipitation changes for seven regions indicated in Fig. 8. *Blue bars* (*bottom*) % precipitation change, *4 colored bars* (*top*) relative contribution of each regime change to precipitation decrease. *Negative bar* indicates that change in that particular regime contributes to more precipitation to the region

century are equal to 4.5, 6.5, 4.5 and 4 days, respectively, indicating longer lasting events of anticyclonic regime in the twenty-first century. More specifically, during the period 2021-2050, the anticyclonic regime, in addition of becoming more frequent, events are on average longer lived. Even more, shorter events (less than 6 days) decrease while longer lasting events (>10 days) increase. The effect on temperature is therefore longer lasting positive temperature anomalies over most of the (western) region, as well as more frequent and longer lasting negative precipitation anomalies in most of the region. Although the relative frequency of meridional WR is not projected to change in this simulation, the mean duration of events does increase, with a larger tail of long-lived events. This implies longer-lived negative T2 m anomalies, and negative precipitation anomalies in the western part of the basin, and positive precipitation anomalies in the eastern part. Finally, both cyclonic and zonal regime frequencies are projection to decrease, with no significant changes in the duration of these events.

5 Summary and conclusions

We have classified the winter-time synoptic activity over the greater Mediterranean basin via a clusters analysis, and found four distinct weather regimes. The composites of surface and atmospheric variables, namely temperature, precipitation, cloudiness, and radiation fields for these regimes were aproduced to draw the complete picture of each regime. The cluster analysis was done on an observational and modelling basis, using daily 700 hPa geopotential height fields from ERA40 for the period December 1983–February 2000. This period was chosen because it overlaps with the period for which satellite ISCCP daily cloud cover data are available.

The four regimes have been named according to their nature as: cyclonic, anticyclonic, meridional and zonal. The most frequent regime is the anticyclonic one (occurring 28 % of the winter days). It is characterized by a strong positive geopotential anomaly centred over France, and is associated to less than normal cloud cover and negative precipitation anomalies. On the other hand, the least frequent regime is the cyclonic (occurring 22 % of the winter days), having an almost opposite configuration to the anticyclonic regime, with strong negative geopotential height anomalies centred over France, above mean cloud cover and positive precipitation anomalies over most of the domain. Despite its lower frequency of occurrence, between 40 and 60 % of the total winter precipitation falls during days of this regime, indicating the episodic nature of winter precipitation in the region.

The LMDz model reproduces remarkably well the four regimes, the composites of the surface and atmospheric variables. Despite this agreement, however, there is an overestimation of the total seasonal precipitation. The main shortcoming of the LMDz model is the relative occurrence of the different regimes. Whereas LMDz simulates a frequency of about 23 and 25 % for the cyclonic and anticyclonic regimes, respectively, ERA40 indicates frequencies of 22 and 28 % of cyclonic and anticyclonic events respectively. This partly explains the precipitation overestimation in the model. We conclude from this analysis that circulation anomalies associated with the four predominant weather regimes, are a dominant controlling factor for the climate in the Mediterranean region, at least during winter.

Climate change projection for the Mediterranean using the LMDz model, indicates an important surface warming in 2021–2050, with a south-west/north-east gradient, from about 1.5 degree to up to 4 degrees. The south-west/north-east gradient is also seen in the ensemble of ENSEMBLES-RCM projections (Déqué et al. 2012) and also in the CMIP3 ensemble (Giorgi and Lionello (2008); Mariotti et al. 2008). The LMDz temperature projection by mid-twenty-first century is similar to the projected warming in the driving model, except over the Mediterranean See, where LMDz simulates between 0.5 and 1 °C less warming.

The cluster analysis for the future period indicates small but statistically significant changes in the relative frequency of occurrence of three of the four weather regimes. Anticyclonic weather regime increases and the cyclonic and zonal regimes decrease. These changes, together with changes in WR intensity, and event length or duration can explain part of the simulated temperature and precipitation

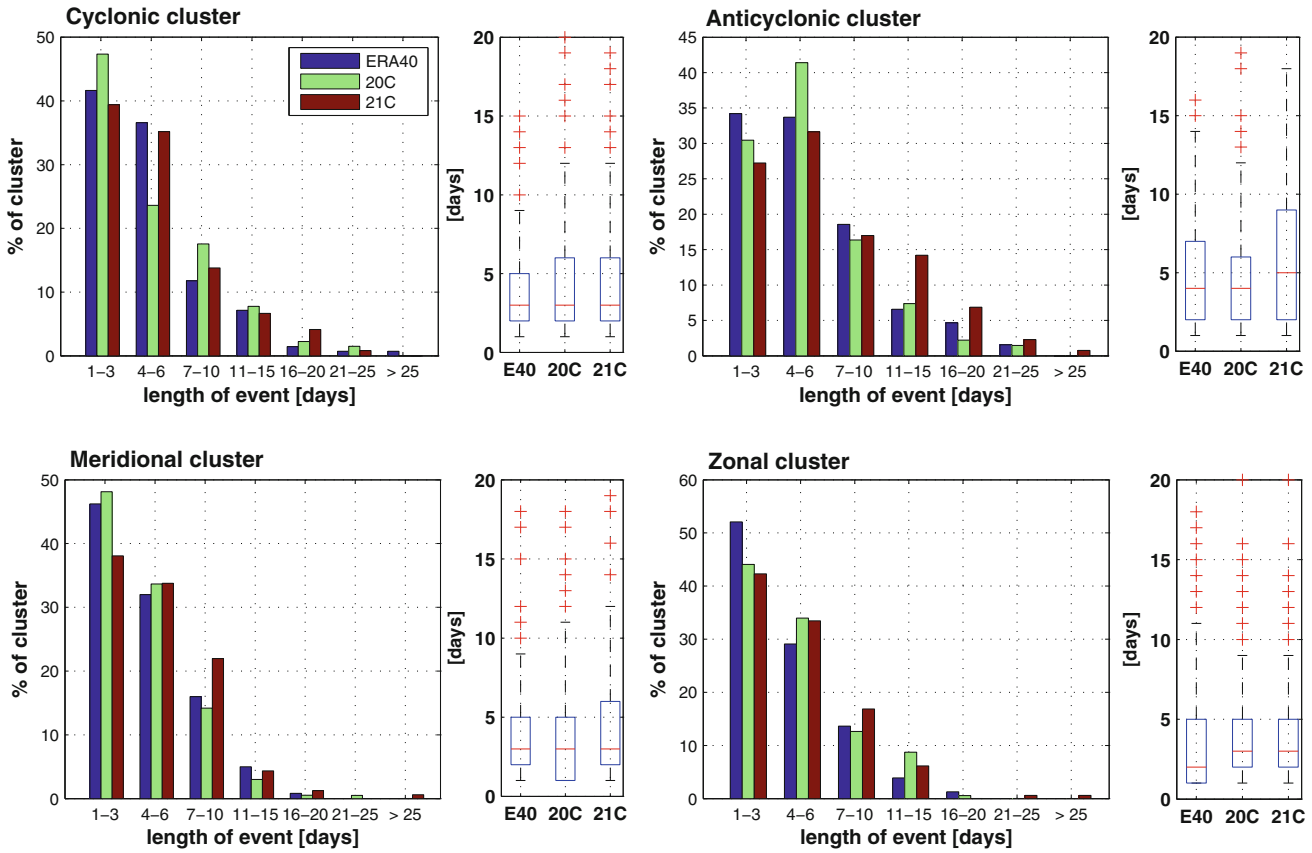

Fig. 10 Histogram of frequency distribution of the length (in days) of events, namely series of days characterized by a specific weather regime, of each one of the four Mediterranean weather regimes. Values are expressed in % of the total frequency of occurrence of each weather regime. Results are given separately for the twentieth century (1961–2000, in *green colours*) and twenty-first century (2021–2050, in *brown colours*), ERA40 are also given for reference (*blue bars*). White histograms, at the *right* of each plot, shows the mean duration of each WR in the twentieth and in the twenty-first centuries

changes over the Mediterranean region. It should be stressed that the fact that the regime frequency and event length changes, has non negligible implications for the validity of statistical downscaling of GCMs, which often need to assume stationarity in these variables, and hence give support to the use of Regional Climate Models for regional Climate change studies. A similar result is reported in Driouech et al. (2010) for Morroco.

The results of our LMDz simulation for the twenty-first century, confirm the already alarmed desertification in the Mediterranean semi-arid and arid regions, including most parts of the Iberian, Italian and Greek Peninsulas (e.g. Alcamo et al. 2007). Understanding of the causes of this desertification is of major importance, given its environmental, economic and social impacts. Our analysis provides a primary mechanism giving a first order explanation of this future desertification. This is in the modified frequency of occurrence of the main weather regimes prevailing over the Mediterranean region during winter, and the expected changing weather conditions above it. Further investigation is needed in order to clarify the reasons for the specific changes in synoptic conditions and atmospheric circulation and the share of natural and anthropogenic forcing agents in these changes.

Acknowledgments Support by the European Union Integrated Project -036961, Climate Change and Impact Research: the Mediterranean Environment (CIRCE) is acknowledged. This work was partly supported by the French ANR project REMEMBER (ANR-12-SENV-0001).

References

Alcamo J et al (2007) Europe. Climate change 2007: impacts, adaptation and vulnerability. Contribution of working group II to the fourth assessment report of the intergovernmental panel on climate change, M. L. Parry, O. F. Canziani, J. P. Palutikof, P. J. Van der Linden and C. E. Hanson, Eds., Cambridge University Press, Cambridge, UK, 541–580

Alpert P et al (2006) Relations between climate variability in the Mediterranean region and the tropics: ENSO, South Asian and African monsoons, hurricanes and Saharan dust. In: Lionello P, Malanotte-Rizzoli P, Boscolo R (eds) Mediterranean climate variability. Elsevier, Amsterdam, pp 149–177

Beaulant AL, Joly B, Nuissier O, Somot S, Ducrocq V, Joly A, Sevault F, Deque M, Ricard D (2011) Statistico-dynamical downscaling for Mediterranean heavy precipitation. Q J R Meteorol Soc 137:736–748

Christensen JH et al (2007) Regional climate projections. Climate change 2007: The physical science basis. Contribution of working group I to the fourth assessment report of the Intergovernmental panel on climate change. In: Solomon S, Qin D, Manning M, Chen Z, Marquis M, Averyt KB, Tignor M, Miller HL (eds). Cambridge University Press, Cambridge, United Kingdom and New York, NY

Coppola E, Giorgi F, Rauscher SA, Piani C (2010) Model weighting based on mesoscale structures in precipitation and temperature in an ensemble of regional climate models. Clim Res 44:121–134. doi:10.3354/cr0094

Corti S, Molteni F, Palmer TN (1999) Signature of recent climate change in frequencies of natural atmospheric circulation regimes. Nature 398:799–802

Déqué M, Somot S, Sanchez-Gomez E, Goodess C, Jacob D, Lenderink D, Christensen OB (2012) The spread amongst ENSEMBLES regional scenarios: regional climate models, driving general circulation models and interannual variability. Clim Dyn 38:951–964. doi:10.1007/s00382-011-1053-x

Driouech F, Déqué M, Sánchez-Gómez E (2010) Weather regimes—Moroccan precipitation link in a regional climate change simulation. Global Planet Change 72(2010):1–10. doi:10.1016/j.gloplacha.2010.03.004

Fontaine B, Gaetani M, Ullmann A, Roucou P (2011) Time evolution of observed July-September sea surface temperature-Sahel climate teleconnection with removed quasi-global effect (1900–2008). J Geophys Res 116:D04105. doi:10.1029/2010JD014843

Giorgi F (2006) Climate change hot-spots. Geophys Res Lett 33:L08707

Giorgi F, Lionello P (2008) Climate change projections for the Mediterranean region. Global Planet Change 63:90–104

Hatzianastassiou N, Gkikas A, Mihalopoulos N, Torres O, Katsoulis BD (2009) Natural versus anthropogenic aerosols in the eastern Mediterranean basin derived from multiyear TOMS and MODIS satellite data. J Geophys Res 114:D24202. doi:10.1029/2009JD011982

Haylock MR, Hofstra N, Klein Tank AMG, Klok EJ, Jones PD, New M (2008) A European daily high-resolution gridded data set of surface temperature and precipitation for 1950–2006. J Geophys Res 113:D20119. doi:10.1029/2008JD010201

Hourdin F, Musat I, Bony S, Braconnot P, Codron F, Dufresne JD, Fairhead L, Filiberti MA, Friedlingstein P, Grandpeix J, Krinner G, LeVan P, Li ZX, Lott F (2006) The LMDZ4 general circulation model: climate performance and sensitivity to parametrized physics with emphasis on tropical convection. Clim Dyn 27:787–813. doi:10.1007/s00382-006-0158-0

Hurrell J (1996) Influence of variations in extratropical wintertime teleconnections on Norhtern Hemisphere temperature. Geo Res Lett 23(6):665–668

Jones PD, Lister DH (2009) The influence of the circulation on surface temperature and precipitation patterns over Europe. Clim Past 5:259–267

L'Hévéder B, Li L, Sevault F, Somot S (2012) Interannual variability of deep convection in the Northwestern Mediterranean simulated with a coupled AORCM. Clim Dyn. doi:10.1007/s00382-012-1527-5

Li Z (1999) Ensemble atmospheric GCM simulation of climate interannual variability from 1979 to 1994. J Clim 12:986–1001

Lionello P et al (2006a) The Mediterranean climate: an overview of the main characteristics and issues. In: Lionello P, Malanotte-Rizzoli P, Boscolo R (eds) Mediterranean climate variability. Elsevier, Amsterdam, pp 1–26

Lionello P et al (2006b) Cyclones in the Mediterranean region: climatology and effects on the environment. In: Lionello P, Malanotte-Rizzoli P, Boscolo R (eds) Mediterranean climate variability. Elsevier, Amsterdam, pp 325–372

Luterbacher J et al (2006) Mediterranean climate variability over the last centuries. A review. In: Lionello P, Malanotte-Rizzoli P, Boscolo R (eds) Mediterranean climate variability. Elsevier, Amsterdam, pp 27–148

MacQueen JB (1967) Some Methods for classification and analysis of multivariate observations. in: Proceedings of 5th Berkeley symposium on mathematical statistics and probability. University of California Press. pp. 281–297. MR0214227. Zbl 0214.46201. http://projecteuclid.org/euclid.bsmsp/1200512992

Mariotti A, Zeng N, Yoon JH, Artale V, Navarra A, Alpert P, Li L (2008) Mediterranean water cycle changes: transition to drier twenty-first century conditions in observations and CMIP3 simulations. Environ. Res. Lett. 3 044001. doi:10.1088/1748-9326/3/4/044001

Marti O et al (2010) Key features of the IPSL ocean atmosphere model and its sensitivity to atmospheric resolution. Clim Dyn 34:1–26. doi:10.1007/s00382-009-0640-6

MEDATLAS (1997) Mediterranean hydrological Atlas on CD- ROM. IFREMER (Ed.), published by IFREMER/DITI/IDT on behalf of the MEDATLAS consortium under contract MAS2-CT93-0074

Michelangeli P, Vautard R, Legras B (1995) Weather regimes: recurrence and quasi-stationarity. J Atmos Sci 52:1237–1256

Moron V, Plaut G (2003) The impact of El Niño southern oscillation upon weather regimes over Europe and the North Atlantic boreal winter. Int J Climatol 23:363–379

Nuissier O, Joly B, Joly A, Ducrocq V, Arbogast P (2011) A statistical downscaling to identify the large-scale circulation patterns associated with heavy precipitation events over southern France. Q J R Meteorol Soc 137:1812–1827

Plaut G, Simmonnet E (2001) Large-scale circulation classification, weather regimes, and local climate over France, the Alps and Western Europe. Clim Res 17:303–324

Rayner NA, Parker DE, Horton EB, Folland CK, Alexander LV, Rowell DP, Kent EC, Kaplan A (2002). Global analyses of sea surface temperature, sea ice, and night marine air temperature since the late nineteenth century J Geophys Res 108(D14):4407. doi:10.1029/2002JD002670

Rojas M (2006) Multiple nested regional climate simulations for Southern South America: sensitivity to model resolution. Mon Weather Rev 134:2208–2223

Rossow WB, Garder LC (1993) Cloud detection using satellite measurements of infrared and visible radiances for ISCCP. J Clim 6:2341–2369

Rossow WB, Golea V (2013) Factors that might affect ISCCP determinations of long-term cloud cover changes. J Climate (submitted)

Rossow WB, Schiffer RA (1999) Advances in understanding clouds from ISCCP. Bull Am Meteorol Soc 80:2261–2288

Rossow WB, Walker AW, Beuschel DE, Roiter MD (1996) International satellite cloud climatology project (ISCCP) Documentation of new cloud datasets. WMO/TD-No. 737, World Meteorological Organization

Rousseeuw PJ (1987) Silhouettes: a graphical aid to the interpretation and validation of cluster analysis. Comput Appl Math 20:53–65. doi:10.1016/0377-0427(87)90125-7

Santos JA, Corte-Real J, Leite SM (2005) Weather regimes and their connection to the winter rainfall in Portugal. Int J Climatol 25:33–50

Sevault F, Somot S, Beuvier J (2009) A regional version of the NEMO ocean engine on the Mediterranean Sea : NEMOMED8 user's guide, Note 107. Groupe de Météorol. de Grande Echelle et Climat, CNRM, Toulouse

Solman SA, Menéndez CG (2003) Weather regimes in the South American sector and neighbouring oceans during winter. Clim Dyn 21(1):91–104

Straus DM, Molteni F (2004) Circulation regimes and SST forcing: results from large GCM ensembles. J Climate 17:1641–1656

Stubenrauch CJ, Rossow WB, Kinne S, Ackerman S, Cesana G, Chepfer H, Getzewich B, Di Girolamo L, Guignard A, Heidinger A, Maddux B, Menzel P, Minnis P, Pearl C, Platnick S, Riedi J, Sun-Mack S, Walther A, Winker D, Zeng S, Zhao G (2012) Assessment of global cloud datasets from satellites: project and database initiated by the GEWEX radiation panel. Bulletin of the American Meteorological Society. doi:10.1175/BAMS-D-12-00117

Trigo R et al (2006) Relations between variability in the Mediterranean region and mid-latitude variability. In: Lionello P, Malanotte-Rizzoli P, Boscolo R (eds) Mediterranean climate variability. Elsevier, Amsterdam, pp 179–226

Ulbrich U et al (2006) The Mediterranean climate change under global warming. In: Lionello P, Malanotte-Rizzoli P, Boscolo R (eds) Mediterranean climate variability. Elsevier, Amsterdam, pp 398–415

Ullmann A, Moron V (2008) Weather regimes and sea surge variations over the Gulf of Lions (French Mediterranean coast) during the 20th century. Int J Climatol 28:159–171. doi:10.1002/joc.1527

Uppala SM et al (2005) The ERA-40 re-analysis. Quart J R Meteorol Soc 131:2961–3012. doi:10.1256/qj.04.176

Valcke S (2006) OASIS3 user guide (oasis3_prism_2-5). PRISM support initiative report no 3. CERFACS, Toulouse, France 64 pp

Vautard R (1990) Multiple weather regimes over the North-Atlantic—analysis of precursors and successors. Mon Wea Rev 118:2056–2081. doi:10.1175/1520-0493

Vrac M, Yiou P (2010) Weather regimes designed for local precipitation modeling: application to the Mediterranean basin. J Geophys Res 115:D12103. doi:10.1029/2009JD012871

Xoplaki E, González-Rouco FJ, Luterbacher J, Wanner H (2004) Wet season Mediterranean precipitation variability. Influence of large-scale dynamics. Clim Dyn 23:63–78

Yiou P, Ribereau P, Naveau P, Nogaj M, Brázdil R (2006) Statistical analysis of floods in Bohemia (Czech Republic) since 1825. Hydrol Sci J 51(5):930–945. doi:10.1623/hysj.51.5.930